ELSEVIER

NeuroImage

www.elsevier.com/locate/ynimg
NeuroImage 21 (2004) 848–857

Why am I unsure? Internal and external attributions of uncertainty dissociated by fMRI

Kirsten G. Volz,* Ricarda I. Schubotz, and D. Yves von Cramon

Max Planck Institute of Cognitive Neuroscience, Leipzig, Germany

Received 7 May 2003; revised 16 October 2003; accepted 21 October 2003

Behavioral evidence suggests that the perceived reason of uncertainty causes different coping strategies to be implemented, particularly frequency ratings with externally attributed uncertainty and memory search with internally attributed uncertainty.

We used functional magnetic resonance imaging (fMRI) to investigate whether processes related to these different attributions of uncertainty differ also in their neural substrates. Participants had to predict events that were uncertain due to internal factors, that is, insufficient knowledge. Data were compared with a preceding study in which event prediction was uncertain due to external factors, that is, event probabilities. Parametric analyses revealed the posterior frontomedian cortex, that is, mesial Brodmann Area 8 (BA 8) as the common cortical substrate mediating processes related to uncertainty no matter what the cause of uncertainty. However, processes related to the two differently attributed types of uncertainty differed significantly in relation to the brain network that was coactivated. Only processes related to internally attributed uncertainty elicited activation within the mid-dorsolateral and posterior parietal areas known to underlie working memory (WM) functions.

Together, findings from both experiments suggest that there is a common cerebral correlate for uncertain predictions but different correlates for coping strategies of uncertainty. Concluding, BA 8 reflects that we are uncertain, coactivated networks what we do to resolve uncertainty.

Keywords: fMRI; Brodmann Area 8; Uncertainty

Introduction

From a deterministic point of view, uncertainty is always caused by a lack of knowledge. Nevertheless, uncertainty can be attributed to different reasons, and these different reasons determine the way we try to resolve our uncertainty, that is, coping strategies. A phenomenological analysis by Kahneman and Tversky (1982) distinguishes between external attribution of uncertainty and internal attribution of uncertainty in decision making, a distinction also made by other authors (e.g., Howell, 1971; Teigen, 1994). External attribution of uncertainty occurs whenever we think that our uncertainty is due to coincidental chance events in a world which we cannot control. As a prominent coping strategy, then, we try to rate the probability of external events (e.g., "There is a 60% chance for rain tomorrow"). Internal attribution of uncertainty, in contrast, occurs whenever we think that our uncertainty is due to a lack or insufficiency of knowledge, that is, to internal factors in ourselves which in principle we could control. A successful coping strategy in this case is an intensive memory search, most likely in combination with an attempt to obtain missing information from valid external sources (e.g., "I am quite sure that possums are mammals, but I don't know exactly"). Accordingly, depending on the perceived cause of uncertainty, frequency ratings or memory searches are used as specific coping strategies in uncertain decision situations.

In a previous experiment (Volz et al., 2003, called Experiment 1 (Exp.1) in the following), we used functional Magnetic Resonance Imaging (fMRI) to investigate strategic processes related to externally attributed uncertainty in decision making. Participants had to predict which of the two concurrently presented stimuli would win in a virtual competition game. Externally attributed uncertainty was manipulated by varying winning probabilities according to specified winning rules. In the present follow-up experiment (Experiment 2 (Exp.2)), we set out to investigate neural correlates of strategic processes related to internally attributed uncertainty in decision making and inasmuch these differ from those related to externally attributed uncertainty. Using the same experimental paradigm as in Exp.1, internally attributed uncertainty was induced by varying the degrees of instructed knowledge about the winning rules. Parallel to Exp.1, where we induced five levels of externally attributed uncertainty, we induced four levels of internally attributed uncertainty in Exp.2.

For processes related to externally attributed uncertainty in Exp.1, activation within the mesial Brodmann Area (BA) 8 increased with increasing uncertainty. Using the same parametric approach as in Exp.1, we set out to investigate if processes related to internally attributed uncertainty are also reflected by activation within frontomedian areas (main effect), and if so, whether this

* Corresponding author. Max Planck Institute of Cognitive Neuroscience, P.O. Box 500 355, Stephanstr. 1A, D-04303 Leipzig, Germany. Fax: +49-341-9940-221.

E-mail address: volz@cns.mpg.de (K.G. Volz).

URL: http://www.cns.mpg.de.

Available online on ScienceDirect (www.sciencedirect.com.)

1053-8119/$ - see front matter © 2004 Elsevier Inc. All rights reserved.
doi:10.1016/j.neuroimage.2003.10.028

activation also increases with increasing internally attributed uncertainty (parametric effect). Hence, we tested the hypothesis that mesial BA 8 activation reflects strategic processes related to increasing uncertainty in decision making, regardless of the reason of uncertainty. In a subsequent group comparison (between-subjects design), we tested the hypothesis whether coping strategies related to internally and externally attributed uncertainty differ concerning other brain activations. Particularly, because storage and retrieval of acquired visuomotor associations are required for the suggested coping strategy in decisions under internally attributed uncertainty (Kahneman and Tversky, 1982), we expected fronto-parietal activations in networks that subserve working memory (WM) functions (Fletcher and Henson, 2001; Owen, 2000).

Methods

Participants

Twelve (seven female, mean age: 25.1, range: 20–31 years) right-handed, healthy volunteers participated in the study. After being informed about potential risks and screened by a physician, subjects gave informed consent before participating. The experimental standards were approved by the local ethics committee of the University of Leipzig. Data were handled anonymously.

Procedure

Participants were instructed immediately before the MRI experiment. In the MRI session, participants were supine on the scanner bed with their right and left index finger positioned on the response buttons. To prevent postural adjustments, the participant's arms and hands were carefully stabilized by tape. In addition, form fitting cushions were used to prevent arm, hand, and head motion. Participants were provided with earplugs to attenuate scanner noise. Visual stimuli were presented with VisuaStim (Magnetic Resonance Technologies, Northridge, USA), over two small TFT monitors placed directly in front of the eyes, simulating a distance to a normal computer monitor of about 100 cm. Immediately before the functional imaging session, participants spent 25 min in the scanner so that they could acclimate to the confinement and sounds of the MR environment. Participants performed a training session during these 25 min.

Stimuli and task

To allow for a comparison between the present Experiment (Exp.2) and the preceding Experiment (Exp.1, see Introduction), only few features of the experimental paradigm were modified. As before, participants had to predict which of the two concurrently presented stimuli would win in a virtual competition game. The crucial difference between the two paradigms was that uncertainty in Exp.1 was manipulated by varying winning probabilities between experimental conditions (from 60% to 100%), whereas uncertainty in Exp.2 was manipulated by varying only the degree of knowledge that participants were provided with regarding 15 winning rules, each of which determining a 100% winning probability as dependent on stimulus features (as explained below). The second difference between Exp.1 and Exp.2 was that experimental conditions were announced by task cues in the present study.

We used the same stimulus material as in Exp.1 (Volz et al., 2003).

Stimuli consisted of comic pictures showing UFO's differing in color, shape, and a figure seated within the UFO. Four different colors, shapes, and comic figures were employed, respectively. Within each trial, two of these stimuli were presented concurrently, one on the right and one on the left side of the screen. Within each stimulus dimension, five possible pairings were generated by combining the four different levels (e.g., within the color dimension, the pairings red-yellow, red-blue, yellow-blue, yellow-green, and blue-green were presented; the sixth pairing, here red-green, was generally skipped to restrict rule complexity (see below)). Participants had their index fingers on a left and a right response button, corresponding to the stimulus presentation positions on the screen.

In the prediction conditions, each stimulus dimension (color, shape, figure) represented a rule group consisting of five different subrules specifying the correct feedback, as listed in Table 1. These 15 rules were valid throughout the experiment, that is, yellow always trumped blue and so on. To induce different levels of uncertainty of knowledge, participants were provided with different amounts of information about these rules. One rule group was trained up to optimal performance before the fMRI session (trained rules condition). A second rule group was verbally instructed at the end of this training session, but not practiced (learned rules condition). The third rule group was neither trained nor verbally instructed so that participants were initially ignorant about this set of rules (explored rules condition). In a fourth prediction condition, participants were asked to test which one out of two rule groups, that is, the trained or the learned rule group, was valid within a given block (tested rules condition). The assignment of stimulus dimension to the rule group was balanced among participants.

In the four prediction conditions (trained, learned, explored, and tested), participants were instructed to press the response button spatially corresponding to the stimulus they excepted to win (e.g., after the task cue "color rules are valid", if the red stimulus will win against the blue, or conversely). In the control condition, pairings showed two identical stimuli (same color, shape, and figure). Three arrows in the middle of the screen indicated which of these two stimuli would win. Participants were asked to simply indicate the stimulus that was indicated by the arrows.

As in Exp.1, rule groups were presented in short blocks of five trials. At the beginning of each block, a verbal cue announced the experimental condition. Within each trial, one pair of stimuli was presented for 2 s during which participants'

Table 1
Listed are the three rule groups which consisted of five different and intransitive subrules

Rule group	Color	Comic figure	Shape
Subrules	Yellow trumps blue	A trumps B	Circle trumps triangle
	Blue trumps red	B trumps C	Triangle trumps quadrant
	Green trumps blue	D trumps B	Ellipse trumps triangle
	Red trumps yellow	C trumps A	Quadrant trumps circle
	Yellow trumps green	A trumps D	Circle trumps ellipse

responses were recorded (see Fig. 1). Presentation was followed by a feedback presented for 1.5 s, showing the winner if the prediction was correct, or showing a masking of both stimuli if the prediction was incorrect. The interblock interval was 5 s. Overall, 15 blocks were presented for each of the four prediction conditions and 12 for the control condition, resulting in 72 blocks or 360 trials altogether. Blocks were presented in randomized order, and the order was also balanced among participants.

An enhancement of the BOLD signal was achieved by employing a jittering which allowed assessment of the BOLD response at different times relative to the event onset. Both the beginning of each block as well as the intertrial interval was jittered. Accordingly, while trial duration (3.5 s) and trial asynchrony (5 s) were kept constant, the intertrial interval (mean duration of 1.5 s) varied by a jittering of 0, 500, 1000, or 1500 ms, respectively, assigned randomly to the trials.

Imaging

Imaging was performed at 3 T on a Bruker Medspec 30/100 system equipped with the standard bird cage head coil. Slices were positioned parallel to the bicommissural plane (AC-PC) with 16 slices (thickness: 5 mm; spacing: 2 mm) covering the whole brain. A set of 2D anatomical images was acquired for each participant immediately before the functional experiment using a MDEFT sequence (256 × 256 pixel matrix). Functional images in plane with the anatomical images were acquired using a single-shot gradient EPI sequence (TE = 30 ms, 64 × 64 pixel matrix, flip angle: 90°, field of view: 19.2 cm) sensitive to BOLD contrast. During each trail, two images were obtained from 16 axial slices at the rate of 2.5 s. In a separate session, high resolution whole brain images were acquired from each participant to improve the localization of activation foci using a T1-weighted 3D-segmented MDEFT sequence covering the whole brain.

Data analysis

The MRI data were processed using the software package LIPSIA (Lohmann et al., 2001). Functional data were corrected for motion artifacts using a matching metric based on linear correlation. To correct for the temporal offset among the slices acquired in one scan, a sinc interpolation based on the Nyquist–Shannon Theorem was applied. A temporal highpass filter with a cutoff frequency of 1/170 Hz was used for baseline correction of the signal and a spatial Gaussian filter with 5.65 mm FWHM was applied. The increased autocorrelation due to filtering was taken into account during statistical evaluation. The anatomical slices were coregistered with the full brain scan that resided in the stereotactic coordinate system and then transformed by linear scaling to a standard size. The transformation parameters obtained from this step were subsequently applied to the functional slices so that the functional slices were also registered into the stereotactic space. Slice gaps were scaled using a trilinear interpolation, generating output data with a spatial resolution of 3 × 3 × 3 mm (27 mm^3).

The statistical evaluation was based on a least-squares estimation using the general linear model (GLM) for serially autocorrelated observations (random effects model) (Aguirre et al., 1997; Worsley and Friston, 1995; Zarahn et al., 1997). An event-related design was implemented, that is, the hemodynamic response function was modeled by the experimental conditions for each stimulus (event = onset of stimulus presentation). The measured signal was described by a convolution of the temporal stimulus distribution and the hemodynamic response function. The design matrix was generated utilizing a synthetic hemodynamic response function and its first and second derivative (Friston et al., 1998) and a response delay of 6 s. The model equation, including the observation data, the design matrix, and the error term, was convolved with a Gaussian kernel with a dispersion of 4 s FWHM. In the following, contrast maps, that is, estimates of the raw-score differences among specified conditions, were generated for each session and subject. As the individual functional datasets were all aligned to the same stereotactic reference space, a group analysis was performed. For multisession analysis, the random-effects analysis can be effected as a one-sample t test on the resulting contrast images across subjects and sessions (Holmes and Friston, 1998; Worsley and Friston, 1995). Subsequently, t values were transformed into z scores. To minimize the probability of false positives (type I error), only voxels with a z score greater than 3.09 ($P < 0.001$ uncorrected) and with a volume greater than 225 mm^3 (5 voxels) were considered as activated voxels (Braver et al., 2001).

Effects of levels of prediction uncertainty were analyzed using a parametric design that paralleled that of Exp.1 (Büchel et al., 1996, 1998; Lange, 1999). To model the effects of prediction uncertainty as a measure of performance, we had used as a regressor the average prediction error per probability of event occurrence in Exp.1. In the present Exp.2, prediction uncertainty was modeled by a regressor consisting of the group-averaged prediction error per experimental condition (trained, learned, explored, and tested). The regressor is called ‘‘condition-regressor’’ in the following. Within the same model, we also controlled for slow unspecific attenuation effects across conditions, that is, for the reduction of condition-independent uncertainty. This was done by introducing a second regressor (called ‘‘attenuation-regressor’’ in the following). Note that the attenuation-regressor could not be modeled individually because attenuation effects depended systematically on the individual presentation order of experimental conditions. To avoid modeling of two statistically interdependent regressors (individual condition-regressor and individual attenuation-regressor), the attenuation-regressor consisted of the group-averaged error score for each trial. Because the order of conditions was balanced interindividually, regressors were statistically independent. By this design, unspecific effects due to a decrease of condition-independent uncertainty could be controlled for. Both condition-regressor and attenuation-regressor referred to the same sample of trials, including all prediction conditions, but excluding the control condition. The control condition was modeled as a separate onset vector within the same model. By including both regressors within one statistical model, contrast maps could be generated that extracted three effects of interest independently from each other: first, the main task effect was investigated by building the contrast between collapsed uncertain prediction conditions and the control condition. Second, the parametric effect of levels of prediction uncertainty was tested using the condition-regressor. Third, the parametric effect of condition-independent uncertainty was tested using the attenuation-regressor. Finally, to investigate whether coping strategies related to internally attributed uncertainty differed significantly from those related to externally attributed uncertainty (group comparison between Exp.1 and 2), contrast images were compared

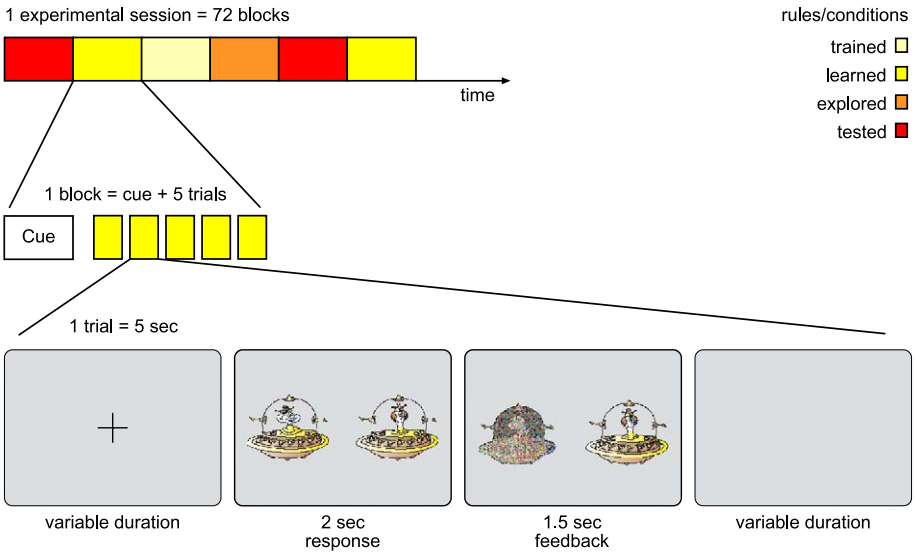

Fig. 1. Example of stimulation. The exemplifying feedback indicates a correct response.

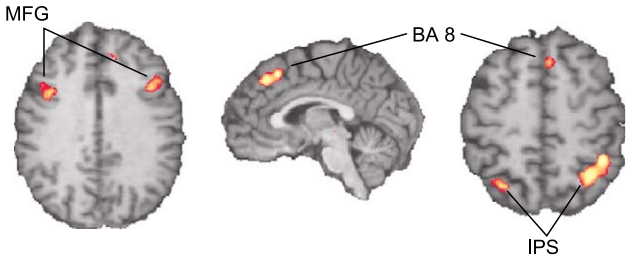

Fig. 2. Main task effect ($Z > 3.09$) for knowledge uncertainty versus certainty (control condition). Group-averaged activations are shown on axial ($z = 32$; 50) and sagittal ($x = 3$) slices of an individual brain normalized and aligned to the Talairach stereotactic space. For activation coordinates, see Table 3. Abbreviations: BA 8, mesial BA 8; MFG, middle frontal gyrus; IPS, intraparietal sulcus.

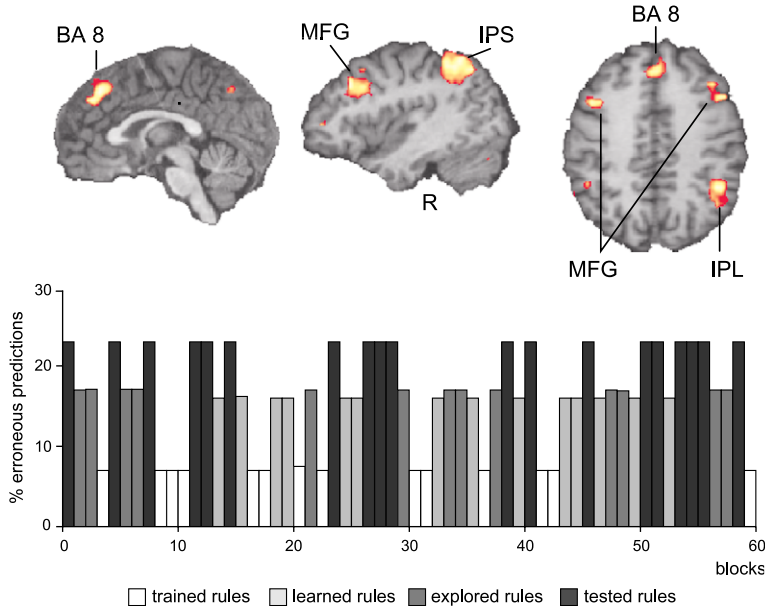

Fig. 3. Parametric effects of knowledge uncertainty. Group-averaged activations of voxels covarying positively with erroneous predictions are shown on sagittal ($x = 1$; 40) and axial ($z = 38$) slices. For activation coordinates, see Table 4. Abbreviations: BA 8, mesial BA 8; MFG, middle frontal gyrus; IPS, intraparietal sulcus; IPL, inferior parietal lobe.

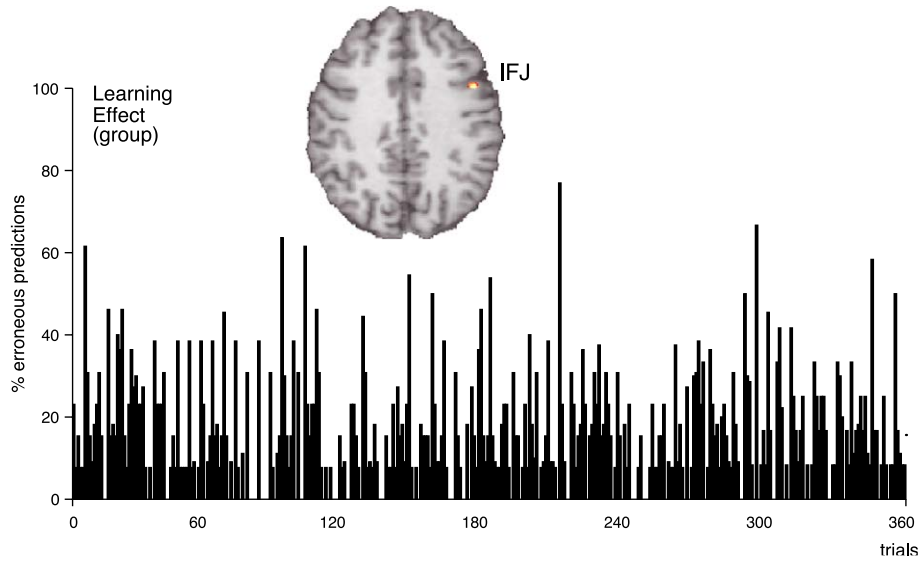

Fig. 4. Parametric effects of slow decreasing uncertainty. Group-averaged activation of voxels covarying positively with the error rates during the experiment is shown on an axial (z = 35) slice. For activation coordinates, see Results section. Abbreviation: IFJ, inferior frontal junction area.

voxelwise using a two-sample t test to examine the hypothesis that the mean contrasts of the two groups differ. The resulting image contains z values indicating the degree of significance of the group difference.

Results

Behavioral data

Performance was measured by the rate of erroneous predictions and reaction times of correct predictions. A repeated measures ANOVA with two-level factor uncertainty (all uncertain conditions collapsed, control condition) yielded a significant main effect both for error rates ($F(1,5) = 35.2$, $P < 0.002$) and for reaction times ($F(1,5) = 61.1$, $P < 0.001$). A repeated measures ANOVA with four-level factor uncertainty (trained, learned, tested, and explored rules) yielded a significant main effect for error rates ($F(3,36) = 14.0$, $P < 0.0001$) but not for reaction times ($F(3,36) = 2.17$, $P = 0.11$) (see Table 2).

Slow unspecific attenuation effects due to a reduction of condition-independent uncertainty were indicated by a significant decrease in reaction times over the course of the experimental session ($F(3,33) = 3.7$; $P = 0.02$) but not by a decrease in error rates ($F(3,33) = 1.0$; $P = 0.39$) which dropped from the first to the last quartile by 4.7%, as compared to 5.5% in Exp.1.

MRI data

Main effect of task

Corresponding to the behavioral analysis, the main task effect was tested by collapsing all uncertain prediction blocks and contrasting them against the control condition (absolute certain prediction). Significant activations were found within the right posterior frontomedian cortex (mesial BA 8), bilaterally within inferior prefrontal areas (inferior frontal junction area (IFJ), i.e., at

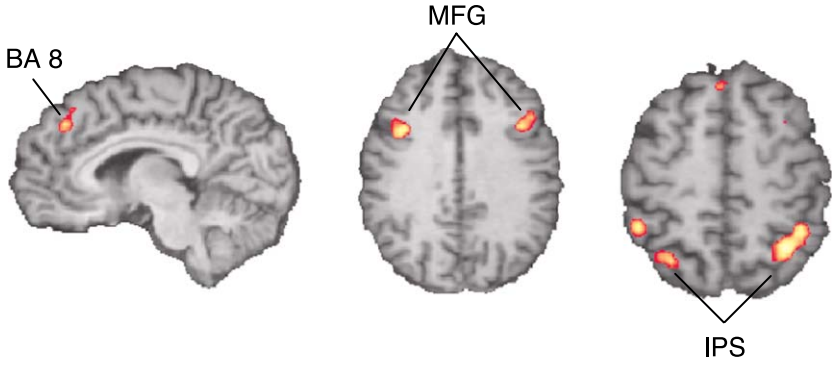

Fig. 5. Group comparison between the two types of uncertainty. Significant differences in activation strength are found within the anterior portion of mesial Brodmann Area 8 (BA 8), the posterior middle frontal gyrus (MFG), and within posterior parietal areas bordering the intraparietal sulcus (IPS). For activation coordinates, see Table 5.

Table 2
Error rates (mean and SD in percent) and reaction times (mean and SD in ms) for the different conditions during the fMRI scanning ($n = 12$)

Rule group	Error rates (%)	Reaction times (ms)
Trained	6.6 (1.9)	881.2 (41.4)
Learned	15.7 (3.5)	901.2 (63.3)
Explored	16.8 (1.9)	878.6 (51.4)
Tested	23.4 (3.8)	1005.2 (55.2)
Control condition	0	617.8 (26.4)

the cross-section of the inferior frontal sulcus and the inferior precentral sulcus), midportions of the middle frontal gyrus (MFG) along the inferior frontal sulcus (IFS), the antero-superior insula, posterior parietal cortices (along the banks of the intraparietal sulcus (IPS)), within pretectal areas, and extrastriate visual cortices (see also Table 3 and Fig. 2).

Effects of levels of uncertainty

Effects of levels of internally attributed uncertainty were tested using the condition-regressor (group-averaged prediction error per experimental condition). As listed in Table 4 and shown in Fig. 3, significant activations were elicited within the right frontomedian cortex (anterior portion of mesial BA 8), the left IJF, the right midportion of MFG, and bilaterally within posterior parietal cortices along the banks of the anterior portion of the IPS. Note that trials with correct and incorrect responses were collapsed because excluding the trials with negative feedback did not change the overall activation pattern, except for a little worse signal-to-noise ratio. Moreover, when using reaction times as values for the condition-regressor, the same cerebral network was found to be activated. In this case, the overall signal-to-noise ratio was lower than the error-based analysis.

Table 3
Anatomical specification, hemisphere, Talairach coordinates (x,y,z), and maximal z scores ((Z) based on a random effects analysis) of significantly activated voxels in prediction under uncertainty (all levels collapsed) in contrast to prediction under certainty (control condition)

Area	Hemisphere	x	y	z	Z
Frontomedian cortex (mesial BA 8)	R	4	21	47	4.5
Frontomedian cortex (anterior BA 8)	R	1	33	41	4.2
Inferior frontal junction area (IFJ)	L	−38	9	32	3.8
Inferior frontal junction area (IFJ)	R	40	13	32	3.7
Middle frontal gyrus (MFG)	L	−44	25	23	4.4
Middle frontal gyrus (MFG)	R	37	27	26	4.4
Anterior–superior insula	L	−26	24	6	4.5
Anterior–superior insula	R	28	22	9	4.0
Intraparietal sulcus (IPS)	L	−26	−62	50	3.8
Intraparietal sulcus (IPS)	R	31	−53	47	4.6
Pretectal area	L	−5	−29	0	3.8
Pretectal area	R	4	−26	0	3.3
Extrastriate visual cortex	L	−35	−54	−9	4.3
Extrastriate visual cortex	R	31	−50	−8	4.3

Table 4
Anatomical specification, hemisphere, Talairach coordinates (x,y,z), and maximal z scores ((Z) based on a random effects analysis) of voxels covarying positively with increasing prediction uncertainty

Area	Hemisphere	x	y	z	Z
Frontomedian cortex (anterior portion of BA 8)	R	1	33	41	4.3
Inferior frontal junction area (IFJ)	L	−44	12	38	4.0
Middle frontal gyrus (MFG)	R	40	24	35	4.2
Inferior parietal sulcus (IPS)	L	−38	−42	44	4.1
Inferior parietal sulcus (IPS)	R	40	−53	50	4.2

Unspecific attenuation effects across the experimental session

We tested for slow unspecific effects that were due to a reduction of condition-independent uncertainty on the BOLD contrast by using the attenuation-regressor (group-averaged error score for each trial). Activations were found within the right IFJ (Talairach coordinates: $x = 46$, $y = 7$, $z = 35$; $Z = 4.0$), the right inferior frontal sulcus (Talairach coordinates: $x = 43$, $y = 15$, $z = 26$; $Z = 3.8$), the left dorsal thalamic system (Talairach coordinates: $x = -14$, $y = -27$, $z = 0$; $Z = 3.7$), and within the right insula (Talairach coordinates: $x = 40$, $y = -5$, $z = -6$; $Z = 3.6$) (see also Fig. 4).

Coping strategies for externally or internally attributed uncertainty

Subsequently, it was tested whether networks underlying coping strategies for externally attributed uncertainty and internally attributed uncertainty differ significantly. A between-subjects group comparison was calculated using a two-sample t test, that is, the two sets of contrast images from Exp.1 and Exp.2 were compared voxelwise (Lohmann et al., 2001). The resulting image (see Fig. 5) contains z values that indicate significant group differences of main task effects. According to our hypotheses, we focused on three regions of interest: the mesial BA 8, frontolateral, and posterior parietal areas. As expected, the inferior

Table 5
Anatomical specification, hemisphere, Talairach coordinates (x,y,z), and maximal z scores ((Z) based on a random effects analysis) indicating the degree of significance of the group difference for internally attributed uncertainty

Area	Hemisphere	x	y	z	Z
Frontomedian cortex (anterior portion of BA 8)	L	−2	31	47	4.0
Inferior frontal junction area (IFJ)	L	−41	18	35	4.2
Inferior frontal junction area (IFJ)	R	40	13	32	3.8
Middle frontal gyrus (MFG)	L	−41	25	23	4.2
Inferior parietal sulcus (IPS)	L	−29	−62	50	3.8
Inferior parietal sulcus (IPS)	L	−47	−44	50	4.0
Inferior parietal sulcus (IPS)	R	31	−53	47	4.7

frontal cortex (IFJ bilaterally; midportion of left MFG/IFS) and posterior parietal cortices correlated positively with processes related to uncertainty when internally attributed. Talairach coordinates were nearly identical to coordinates of the main effect (see Table 5). The number of significantly activated voxels indicating a difference within the anterior portion of mesial BA 8 was negligible (11 voxels) and restricted to the most anterior part of this region.

Discussion

The presented fMRI study was designed to investigate whether processes that are related to different attributions of uncertainty in a prediction task are reflected within the same brain areas. By using a parametric approach and inducing different degrees of uncertainty, we aimed to identify and compare brain correlates of strategic processes related to internally attributed uncertainty (Exp.2) with those related to externally attributed uncertainty (Volz et al., 2003). As a common cortical substrate of processes related to uncertain predictions, regardless of uncertainty attribution, we found the mesial BA 8 to be significantly activated. In contrast, activation within other brain areas differed significantly between the two differently attributed types of uncertainty. A between-subjects comparison showed that processes related to internally attributed uncertainty specifically engaged a fronto-parietal network bilaterally. In the following, both commonly activated brain areas as well as areas that were exclusively activated for processes related to internally attributed uncertainty will be discussed.

Types of uncertainty—or ways of learning, rule validity, and coping strategies?

First, the argument has to be considered that Exp.1 and Exp.2 differed not only concerning differently attributed uncertainties, but also about different types of learning, and also about differently valid stimulus-response rules (SR-rules). As will be argued in the following, however, neither of these two potential confounds can explain the differences between the experiments.

Considering the learning characteristics, externally attributed uncertainty or uncertainty of frequency, respectively, is observed in situations in which we typically cannot learn up to optimal performance, whereas internally attributed uncertainty or uncertainty of knowledge, respectively, emerges if we can, and hence is a transient phenomenon as in contrast to the former. To balance this inherent difference between both types of uncertainty, we manipulated learning requirements in a way that Exp.2 was too short to allow for learning up to optimal performance. Data support that this manipulation was successful: errors decreased from quartile 1 to quartile 4 by 5.5% in Exp.1, and 4.7% in Exp.2. Both learning effects were not significant ($F(3,45) = 2.9$, $P = 0.05$; $F(3,33) = 1.0$, $P = 0.39$, respectively). Therefore, it can be assumed that differences between Exp.1 and Exp.2 cannot be reduced to processes related to the remaining uncertainty in the latter and nonremaining uncertainty in the former.

Considering the second potential confound, rule validity was necessarily the instrument to implement different levels of uncertainty of frequency in Exp.1, in contrast to Exp.2. Following the average rule, validity differed between Exp.1 (80%) and Exp.2 (100%). However, if differences between Exp.1 and 2 were caused by differently valid rules, then one would also expect for the same reason that, firstly, WM networks should not covary parametrically with levels of uncertainty in Exp.2, because they all refer to the same (100%) rule validity; and secondly, that the very same WM networks should be activated and covary parametrically with levels of uncertainty in Exp.1, because they differ concerning rule validity (60%, 70%, 80%, 90%, and 100%). As evident from our data, however, neither is the case. Therefore, rule validity cannot be the cause for systematic differences between Exp.1 and Exp.2.

In contrast, it is of course correct to say that the studies differed concerning the coping strategies they induced, and that these different strategies are reflected by different cerebral activations. Behaviorally, different coping strategies have been suggested to be an indicator for different attributed uncertainties (Kahneman and Tversky, 1982). The term "types of uncertainty" is meant to refer to exactly this definition, that is, different ways to try to resolve decision uncertainty and hence different strategies to avoid future errors or achieve future rewards. Note that the performance scores in both experiments confirmed that participants tried to perform well. This of course had to be proved statistically in particular for Exp.1, where expected maximal performance were below 100% correct responses. To this end, we calculated the discrimination index P_r by P_r = hit-false alarm (Snodgrass and Corwin, 1988). This index allows correcting performance scores for guessing tendencies in all response classes. As a result, all conditions showed to be significantly different from chance level (100%: $t_{(15)} = 37.7$, $P < 0.001$; 90%: $t_{(15)} = 22.3$, $P < 0.001$; 80%: $t_{(15)} = 16.4$, $P < 0.001$; 70%: $t_{(15)} = 7.8$, $P < 0.001$; 60%: $t_{(15)} = 2.2$; $P = 0.04$). Therefore, we can exclude that differences between Exp.1 and Exp.2 were caused by guessing tendencies in the former as in contrast to the latter.

Finally, it is important to note that the present as well as the preceding experiment was not designed to differentiate pre- and postfeedback processes. Although others have tried to disentangle these two processes, it revealed that expectancy and previous experience mostly share common neural substrates (Breiter et al., 2001), as already suggested by behavioral data (Mellers et al., 1997, 1999).

Attribution-independent activation of uncertainty: mesial BA 8

Both strategic processes related to internally as well as to externally attributed uncertainty elicited activation within mesial BA 8 (Talairach coordinates in Exp.1: $x = 8$, $y = 18$, $z = 46$). A group comparison revealed no significant difference in the mean activation value within the posterior part of mesial BA 8. Processes related to internally attributed uncertainty elicited activation within a larger area than those related to externally attributed uncertainty, extending into anterior mesial BA 8 and reaching the border of mesial BA 9. However, this difference was probably caused by a slightly larger activation in Exp.2 and may reflect quantitative rather than qualitative differences.

Like adjacent mesial areas BA 6 (presupplementary motor area, pre-SMA) and adjacent portions of BA 32/24, mesial BA 8 has been repeatedly found in tasks that investigate uncertainty-related processes. In this context, BA 32 (together with BA 24) is usually called the anterior cingulate cortex (ACC). Because the anatomical and functional organization of mesial BA 8 has begun to be focused on only recently, empirical evidence for a functional distinction among these three areas is still weak. Moreover, activations within mesial BA 8 and pre-SMA are difficult to disentangle due to missing macroscopical landmarks among these

areas, and the same applies to the distinction among these regions and ACC. However, because it is widely accepted that laminar differentiations reflect functional differentiations of the cortex, it can be suggested that the considered areas underly different aspects in behavior under uncertainty. For instance, mesial BA 8 is a granular prefrontal isocortex, whereas ACC can be subdivided into agranular (BA 24) and dysgranular (BA 32) cortex.

In view of existing data, however, it appears that mesial BA 8 on one hand and BA 32/24 on the other seem to be preferentially engaged in different experimental paradigms on uncertainty. We will outline this view in the following (see also Volz et al., 2003).

Studies on conflict that report BA 32/24 (often in company with pre-SMA) typically use paradigms such as , for example, the Eriksen flankers task or go/no go tasks (e.g., Bunge et al., 2002; Garavan et al., 2002; Luks et al., 2002; Ruff et al., 2001; Ullsperger and von Cramon, 2001, 2003). Common features of these paradigms are (a) SR-rules are simple (one-to-one mappings), often spatially compatible, and usually known and instructed beforehand, (b) two response tendencies are activated concurrently, so that conflict arises on the response level, (c) errors are usually induced by time pressure and perceptual difficulty, (d) conflict can be diminished by a close stimulus inspection, and (e) feedback evaluation allows to improve performance in perceptual and motor skills. In these paradigms, either ACC or pre-SMA is differently engaged in two subprocesses of conflict, as can be stressed by contrast building. The ACC is predominantly reported in error monitoring (Bunge et al., 2002; Garavan et al., 2002; Kiehl et al., 2000; Ullsperger and von Cramon, 2001), whereas BA 6 or pre-SMA (sometimes extending into mesial BA 8) is rather reflecting conflict detection (Kiehl et al., 2000; Ruff et al., 2001; Ullsperger and von Cramon, 2001). Based on these findings, the functional dissociation between pre-SMA and ACC has become a focus of research (Ullsperger and von Cramon, 2001, 2003) and was confirmed in a recent meta-analysis by Fassbender et al. (2003).

In contrast, ACC activation is typically absent in a different type of paradigm regarding conflict that report mesial BA 8 activation. These studies investigated hypothesis testing with low restrictions (Elliott and Dolan, 1998), the application of arbitrary SR-rules (Goel and Dolan, 2000), and the detection of arbitrary SR-rules (Knutson et al., 2003; Volz et al., 2003). Common features of these are (a) SR-rules are complex (many-to-many mappings), arbitrary, and usually unknown beforehand, (b) decisions tendencies depend on previously evaluated feedbacks, so that conflict arises on the knowledge level, (c) errors are not induced by time pressure, but by cognitive difficulty, (d) conflict can be diminished by mnemonic search, and (e) feedback evaluation allows to improve performance in cognitive skills and knowledge. Speculating on this issue, activation within BA 8 may not be found in many studies investigating uncertainty-related processes because the employed paradigms do not meet the criteria of the latter profile (Bush et al., 2002; Casey et al., 2000; Paulus et al., 2001, 2002).

Together, we conclude that the specific profile of an experimental paradigm determines the type of uncertainty that is experienced and attributed. Depending on the respective causation of uncertainty, different coping strategies are required to resolve uncertainty. The three determinants of uncertain decision situations—cause of uncertainty, effect of uncertainty, and appropriate coping strategy—are necessarily associated. In fact, behaviorally different coping strategies are used to distinguish different causes and effects of uncertainty (compare Kahneman and Tversky, 1982). However, future imaging studies have to test the proposed distinction directly by comparing the two prototypes of paradigms as to the their specific cerebral correlates.

In summary, we suggest both Exp.1 and Exp.2 to draw rather on BA 8 than on ACC (BA 32/24) because the employed tasks correspond to a specific profile of paradigms, that is, deliberate choices based on mnemonic searches, as in contrast to forced responses based on perceptual cues (see above differentiation). To put it shortly, BA 8 and ACC may distinguish "decision conflicts" from "response conflicts". Considering a distinction proposed by Reason (1990), these could be suggested to precede "mistakes" in the former and "action slips" in the latter case.

Attribution-dependent activation of uncertainty

In addition to activation within mesial BA 8, significant activations within MFG, IFJ, and IPS were found to be significantly activated with processes related to internally attributed uncertainty versus control condition. The same sample of areas was found to increase with increasing internally attributed uncertainty (parametric effect) and in direct contrast between processes related to internally attributed and those related to externally attributed uncertainty (Exp.2 vs. Exp.1). These findings confirm our hypothesis that coping strategies related to internally attributed uncertainty, that is, memory search, will engage brain areas subserving WM functions.

The MFG (BA 46/9) is also called mid-dorsolateral prefrontal area (Petrides, 2000). Activations within this region have been reported when monitoring and manipulation of information within WM are required (D'Esposito et al., 1998). The monitoring of mnemonic information is taken to be the key feature of tasks activating mid-dorsolateral prefrontal areas (Petrides, 2002). In our case, mnemonic information are SR-rules that were defined by different nonspatial object properties. The mid-dorsolateral prefrontal coordinates in the present study fit nicely to those reported for nonspatial WM in a recent meta-analysis by Owen (2000) (Talairach coordinates right: 35,32,19; left: −42,23,19).

The manipulation of actively maintained information within WM is suggested to rely on mid-dorsolateral prefrontal cortex (Hartley and Speer, 2000; Petrides, 2002). Accordingly, we take increasing activity within these areas to reflect increasing demands in computations on stored information, specifically the reduction of all possible SR-rules to a smaller set of valid SR-rules. In the case of trained rules, the cue referred to five valid SR-rules concerning property X (e.g., comic figure). In the case of learned rules, participants knew that the cue referred to five valid SR-rules concerning property Y (e.g., color), but not to which exactly. In the case of explored rules, participants knew that the cue referred to five valid SR-rules, but not to which property they applied. Finally, whenever participants had to test whether either the trained or the learned rule-group was valid, the range of to-be-checked SR-rules was twice as large as in the trained or learned rules condition. Hence, we take parametric variations of the mid-dorsolateral prefrontal activation to reflect different requirements on reducing the range of potential SR-rules.

In addition to MFG, we found posterior parietal areas (IPS) to be coactivated, typical for WM functions (Owen, 2000). In contrast to the prefrontal components of this network, the posterior parietal areas are taken to maintain all SR-rules that are valid in an

experiment (Bunge et al., 2002). From this set, currently valid SR-rules are selected by corresponding prefrontal sites (Miller and Cohen, 2001; Smith and Jonides, 1999). By manipulating the number of SR-rules (sample sizes) with which participants started the present study, experimental conditions differed in their requirement to maintain SR-rules, and therefore draw differently on posterior parietal areas.

Regarding IFJ activation, it has been shown that implementation of learned SR-rules elicits activation within the this area (Brass and von Cramon, 2002; Nagahama et al., 2001). This interpretation can be applied to IFJ activation in our study, where selection and implementation of appropriate SR-rules are required throughout the experiment and covary as a function of SR-knowledge. Activation was found to decrease within the same or closely adjacent areas during the experimental session (Fig. 4). This effect replicated findings from Exp.1, though coordinates differed slightly. As discussed in the previous study, we interpret a decrease in IFJ activation to reflect a decrease in effort in implementing valid SR-rules. The same explanation applies to the parametric modulations of IFJ area: as the range of potentially valid SR-rules is reduced, IFJ activation decreases. Note that activation modulation in IFJ cannot be attributed to retrieval success, because increasing success would be reflected in a negative covariation with decreasing IFJ response.

Conclusion

Together with a preceding study (Volz et al., 2003), present data demonstrate that predictions under uncertainty engage mesial BA 8. However, coping strategies for externally attributed uncertainty elicited activations within a dopaminergic subcortical network, and those for internally attributed uncertainty induced activations within a fronto-parietal network. Concluding, mesial BA 8 reflects that we are uncertain, additional networks what we do to resolve uncertainty.

Acknowledgments

We very much thank two anonymous reviewers for helpful feedback on a prior draft, Shirley-Ann Rüschemeyer for revision of the manuscript concerning the language, Markus Ullsperger for constructive comments on the manuscript, Karsten Müller, Andre Szameitat, and Stefan Zysset for support in fMRI statistics, and Andrea Gast-Sandmann for the stimulus material.

This work was supported by the German Research Foundation (SPP 1107).

References

Aguirre, G.K., Zarahn, E., D'Esposito, M., 1997. Empirical analyses of BOLD fMRI statistics: II. Spatially smoothed data collected under null-hypothesis and experimental conditions. NeuroImage 5, 199–212.

Brass, M., von Cramon, Y.D., 2002. The role of the frontal cortex in task preparation. Cereb. Cortex 12, 908–914.

Braver, T.S., Barch, D.M., Kelley, W.M., Buckner, R.L., Cohen, N.J., Miezin, F.M., Snyder, A.Z., Ollinger, J.Z., Akbudak, E., Conture, T.E., Petersen, S.E., 2001. Direct comparison of prefrontal cortex regions engaged in working memory and long-term memory tasks. NeuroImage 14, 48–59.

Breiter, H.C., Aharon, I., Kahneman, D., Dale, A., 2001. Functional imaging of neural responses to expectancy and experiences of monetary gains and losses. Neuron 30, 619–639.

Büchel, C., Wise, R.J.S., Mummery, C.J., Poline, J.-B., Friston, K.J., 1996. Nonlinear regression in parametric activation studies. NeuroImage 4, 60–66.

Büchel, C., Holmes, A.P., Rees, G., Friston, K.J., 1998. Characterizing stimulus-response functions using nonlinear regressors in parametric fMRI experiments. NeuroImage 8, 140–148.

Bunge, S.A., Hazeltine, E., Scanlon, M.D., Rosen, A.C., Gabrieli, J.D.E., 2002. Dissociable contributions of prefrontal and parietal cortices to response selection. NeuroImage 17, 1562–1571.

Bush, G., Vogt, B.A., Holmes, J., Dale, A.M., Greve, D., Jenike, M.A., Rosen, B.R., 2002. Dorsal anterior cingulate cortex: a role in reward-based decision making. Proc. Natl. Acad. Sci. U. S. A. 99, 523–528.

Casey, B.J., Thomas, K.M., Welsh, T.F., Badgaiyan, R.D., Eccard, C.H., Jennings, J.R., Crone, E.A., 2000. Dissociation of response conflict, attentional selection, and expectancy with functional magnetic resonance imaging. Proc. Natl. Acad. Sci. U. S. A. 97, 8728–8733.

D'Esposito, M.D., Aguirre, G.K., Zarahn, E., Ballard, D., Shin, R.K., Lease, J., 1998. Functional MRI studies of spatial and nonspatial working memory. Cogn. Brain Res. 7, 1–13.

Elliott, R., Dolan, R.J., 1998. Activation of different anterior cingulate foci in association with hypothesis testing and response selection. NeuroImage 8, 17–29.

Fassbender, C., Hester, R., Garavan, H., 2003. A review of midline activations associated with error processing and conflict monitoring. NeuroImage 19, S393.

Fletcher, P.C., Henson, R.N.A., 2001. Frontal lobes and human memory. Brain 124, 849–881.

Friston, K.J., Fletcher, P., Josephs, O., Holmes, A., Rugg, M.D., Turner, R., 1998. Event-related fMRI: characterizing differential responses. NeuroImage 7, 30–40.

Garavan, H., Ross, T.J., Murphy, K., Roche, R.A.P., Stein, E.A., 2002. Dissociable executive functions in the dynamic control of behavior: inhibition, error detection, and correction. NeuroImage 17, 1820–1829.

Goel, V., Dolan, R.J., 2000. Anatomical segregation of component processes in an inductive inference task. J. Cogn. Neurosci. 12, 110–119.

Hartley, A.A., Speer, N.K., 2000. Locating and fractionating working memory using functional neuroimaging: storage, maintenance, and executive functions. Microsc. Res. Tech. 51, 45–53.

Holmes, A.P., Friston, K.J., 1998. Generalisability, random effects and population inference. NeuroImage 7, 754.

Howell, W.C., 1971. Uncertainty from internal and external sources: a clear case of overconfidence. J. Exp. Psychol. 89, 240–243.

Kahneman, D., Tversky, A., 1982. Variants of uncertainty. Cognition 11, 143–157.

Kiehl, K.A., Liddle, P.F., Hopfinger, J.B., 2000. Error processing and the rostral anterior cingulate: an event-related fMRI study. Psychophysiology 37, 216–223.

Knutson, B., Fong, G.W., Bennett, S.M., Adams, C.M., Hommer, D., 2003. A region of mesial prefrontal cortex tracks monetarily rewarding outcomes: characterization with rapid event-related fMRI. NeuroImage 18, 263–272.

Lange, N., 1999. Statistical procedures for functional MRI. In: Moonen, C.T.W., Bandettini, P.A. (Eds.), Functional MRI. Springer, Heidelberg, pp. 301–335.

Lohmann, G., Mueller, K., Bosch, V., Mentzel, H., Hessler, S., Chen, L., Zysset, S., von Cramon, D.Y., 2001. LIPSIA—A new software system for the evaluation of functional magnetic resonance images of the human brain. Comput. Med. Imaging Graph. 25, 449–457.

Luks, T.L., Simpson, G.V., Feiwell, R.J., Miller, W.L., 2002. Evidence for anterior cingulate cortex involvement in monitoring preparatory attentional set. NeuroImage 17, 792–802.

Mellers, B., Schwartz, A., Ho, K., Ritov, I., 1997. Decision affect theory: emotional reactions to the outcomes of risky options. Psychol. Sci. 8, 423–429.

Mellers, B., Schwartz, A., Ritov, I., 1999. Emotion-based choice. J. Exp. Psychol. Gen. 128, 332–345.

Miller, E.K., Cohen, J.D., 2001. An integrative theory of prefrontal cortex function. Annu. Rev. Neurosci. 24, 167–202.

Nagahama, Y., Okada, T., Katsumi, Y., Hayashi, T., Yamauchi, H., Oyanagi, C., Konishi, J., Fukuyama, H., Shibasaki, H., 2001. Dissociable mechanisms of attentional control within the human prefrontal cortex. Cereb. Cortex 11, 85–92.

Owen, A.M., 2000. The role of the lateral frontal cortex in mnemonic processing: the contribution of functional neuroimaging. Exp. Brain Res. 133, 33–43.

Paulus, M.P., Zauscher, B., McDowell, J.E., Frank, L., Brown, G.G., Braff, D.L., 2001. Prefrontal, parietal, and temporal cortex networks underlie decision-making in the presence of uncertainty. NeuroImage 13, 91–100.

Paulus, M.P., Hozack, N., Frank, L., Brown, G.G., 2002. Error rate and outcome predictability affect neural activation in prefrontal cortex and anterior cingulate during decision making. NeuroImage 15, 836–846.

Petrides, M., 2000. The role of the mid-ventrolateral prefrontal cortex in working memory. Exp. Brain Res. 133, 44–54.

Petrides, M., 2002. The mid-ventrolateral prefrontal cortex and active mnemonic retrieval. Neurobiol. Learn. Mem. 78, 528–538.

Reason, J., 1990. Human Error. University Press, Cambridge.

Ruff, C.C., Woodward, T.S., Laurens, K.R., Liddle, P.F., 2001. The role of the anterior cingulate cortex in conflict processing: evidence from reverse stroop interference. NeuroImage 14, 1150–1158.

Smith, E.E., Jonides, J., 1999. Storage and executive processes in the frontal lobes. Science 283, 1657–1661.

Snodgrass, J.G., Corwin, J., 1988. Pragmatics of measuring recognition memory: applications to dementia and amnesia. J. Exp. Psychol. Gen. 117, 34–50.

Teigen, K.H., 1994. Variants of subjective probabilities: concepts, norms and biases. In: Wright, G., Ayton, P. (Eds.), Subjective Probability. Wiley, Chichester, pp. 211–238.

Ullsperger, M., von Cramon, D.Y., 2001. A dissociation of error processing and response competition revealed by event-related fMRI and ERP's. NeuroImage 14, 1387–1401.

Ullsperger, M., von Cramon, D.Y., 2003. Error monitoring using external feedback: specific roles of the habenular complex, the reward system, and the cingulate motor area revealed by functional magnetic resonance imaging. J. Neurosci. 23, 4308–4314.

Volz, K.G., Schubotz, R.I., von Cramon, D.Y., 2003. Predicting events of varying probability: uncertainty investigated by fMRI. NeuroImage 19, 271–280.

Worsley, K.J., Friston, K.J., 1995. Analysis of fMRI time-series revisited—Again. NeuroImage 2, 173–181.

Zarahn, E., Aguirre, G.K., D'Esposito, M., 1997. Empirical analyses of BOLD fMRI statistics. NeuroImage 5, 179–197.